Hindawi
Journal of Advanced Transportation
Volume 2020, Article ID 8878346, 15 pages
https://doi.org/10.1155/2020/8878346

WILEY | Hindawi

Research Article

Expansion of the Fundamental Diagram from a Microscopic Multilane Modeling Framework of Mixed Traffic

Mudasser Seraj, Jiangchen Li, and Tony Z. Qiu

Department of Civil and Environmental Engineering, University of Alberta, Edmonton T6G 2R3, Canada

Correspondence should be addressed to Mudasser Seraj; seraj@ualberta.ca

Received 25 June 2020; Revised 28 October 2020; Accepted 4 November 2020; Published 24 November 2020

Academic Editor: Chengxiang Zhuge

Microscopic modeling of mixed traffic (i.e., automaton-driven vehicles and human-driven vehicles) dynamics, particularly car-following, lane-changing, and gap-acceptance, provides the opportunity to gain a more accurate estimation of flow-density relationships for both traditional traffic with human-driven vehicles and different mixed traffic scenarios. Our paper proposes a microscopic framework to model multilane traffic for both vehicle types on shared roadways which sets the stage to explore the capability of macroscopic car-following models in general to explain the fundamental flow-density relationship. Since prior models inadequately represent the fundamental diagram realistically, we propose a rectified macroscopic flow model that can account for the impact of both lane-changing and gap-acceptance. Differentiability, boundary conditions, and flexibility of the proposed model are tested to validate its applicability. Finally, the capability to interpret the flow-density relationship by the proposed model is verified for different mixed traffic scenarios. Although few model parameter values were obtained directly from the simulation input, the rest of the parameters have been calibrated by flow and density outputs from the simulations. The analysis results show a distinct correlation between the proposed model parameters with automation-driven vehicle shares and lane-changing rates of traffic. The findings from this study emphasize the importance of taking complete motion dynamics into account, rather than partial motion dynamics (i.e., car-following) as has been the case in the previous studies, to explain macroscopic traffic flow characteristics, irrespective of the vehicle type.

1. Introduction

The rapid development of Connected and Automated Vehicle (CAV) technology has motivated researchers and practitioners to consider collaborative approaches, such as AutoDrive Challenge by SAE and General Motors [1], to solve traditional transportation problems. Consequently, researchers have been exploring traditional, fundamental concepts of traffic flow theories from new perspectives and questioning the understanding of the concepts in resulting scenarios. With an improved grasp on fundamental concepts of traffic flow and informed decision making, sustainable growth of CAV technology is possible, as is the identification of the optimal combinations of new technology with traditional transportation infrastructure. The resultant paradigm shifts on traffic operational technologies have prompted researchers to determine the limitations of partial motion dynamics (i.e., car-following) in explaining macroscopic features of multilane traffic flow and ask the question of how to complete vehicle motion dynamics could be considered in equilibrium flow models of traditional and mixed traffic. As such, this study attempts to determine the effectiveness of the macroscopic adaptation of a traditional microscopic car-following model (i.e., the Intelligent Driver Model (IDM) [2] in explaining fundamental features of traffic through detailed microscopic multilane modeling. More significantly, this study proposes a newly conceived, realistic traffic flow model that can (i) account for complete motion dynamics (i.e., car-following, lane-changing, and gap-acceptance) and (ii) interpret the transformation of the fundamental diagram in mixed traffic (i.e., Human-Driven (HuD) and Automaton-Driven (AuD) vehicles) scenarios.

A considerable issue in the research findings up to this point is that, while car-following is the dominant maneuver

in traffic flow, the capability of this microscopic feature to explain the relationship of flow with density is debatable. More promisingly, the IDM is a microscopic car-following model that aims to represent the car-following behavior through stimulus-response characteristics of human drivers. Since car-following models such as the IDM can describe steady-state and homogenous conditions, the macroscopic form can be attained from this model through local aggregation. Since IDM-prescribed acceleration is generated from both speed and headway, one can redevelop the fundamental diagram from a speed-spacing diagram of car-following [3]. The initial goal of this research, then, is to assess the proficiency of the derived fundamental diagram in reproducing an actual flow-density relationship. We, then, put forward an inclusive traffic flow model that reflects the complete motion dynamics of traffic, thereby addressing significant shortcomings in the previous efforts. We also explore the suitability of the proposed model to assess the remaining microscopic features. Finally, we analyze varying mixed traffic flow scenarios developed through the multilane microscopic modeling framework for adaptability attributes of the proposed model.

The rest of the paper is organized as follows: the literature review summarizes the findings from leading studies on macroscopic car-following models and their ability to explain the fundamental features of traffic. Additionally, articles exploring mixed traffic scenarios and their implications on both microscopic and macroscopic perspectives are reviewed. The following section provides a detailed description of the microscopic modeling framework that establishes the foundation of this comprehensive study. An in-depth discussion of the limitations of the macroscopic adaptation of the car-following model and a macroscopic model that accounts for complete motion dynamics of vehicles are, then, described in the next section. The functionality of the proposed model when identifying flow-density patterns is evaluated in the penultimate section, followed by the final section summarizing the research findings and contributions to the literature.

2. Literature Review

To review scholarly contributions made by previous studies that correlate with the present one, we chose to divide the review discussion into two segments and address each segment separately. The two segments of review discussion are (a) macroscopic fundamental relations from car-following models and their capability to explain the fundamental diagram and (b) microscopic and macroscopic aspects of mixed traffic. Some remarkable research efforts and studies that coincide with these two topics have been summarized in this section of the paper to provide insight into current research and existing groundwork available to support the research presented here.

Inspired by Greenshield et al.'s [4] single-regime continuity model, many models have been proposed to formulate speed-spacing (microscopic) or flow-density (macroscopic) relationships [5–17]. These models share two commonalities: (1) the variations of traffic states are explained from one specific perspective, either microscopic or macroscopic, and (2) the traffic is assumed to be homogenous. Under the assumption of homogenous traffic, microscopic models can be upscaled to macroscopic traffic flow models. Ni [18] showed this type of expansion by converting the IDM and longitudinal control model, which are microscopic car-following models, to macroscopic fundamental equations through local aggregation. The macroscopic IDM model is capable of generating a realistic flow-density diagram by employing four parameters to obtain a desirable shape with good fitting quality. While Ni did not explore the generated macroscopic models' competence in explaining traffic flow features, our study will utilize the macroscopic adaptation of the IDM for this direction of research. A reversed approach was taken by Duret et al. [19] where the authors simplified the fundamental diagram in an attempt to quantify individual vehicles' speed-spacing relationship. The results indicated that taking individual variability into account could improve the accuracy of vehicle trajectories. Chiabaut et al. [20] proposed a method to calibrate Newell's car-following model parameter [6], eventually assisting in calibrating the macroscopic model from individual observation. The influence of driver behavioral heterogeneity on the capacity drop was studied by Chen et al. [21]. The findings from the study concluded that both the lane-changing maneuver and variations in driver characteristics could reduce the bottleneck discharge rate by 8–23%. Treiber and Kesting [22] proposed a calibration and validation method for car-following models in the microscopic scale. However, the implications of calibrated parameters and its effect on best fit on the fundamental diagram remain unexplored. A similar approach to calibration and validation of car-following models was taken by Zheng et al. [23]. This study provided an intriguing insight into the validation and accuracy of car-following models by suggesting that the inclusion of a higher number of parameters in a car-following model could provide greater accuracy but might overfit in some scenarios. To address this issue, the authors suggested using different parameters and car-following models in different traffic conditions.

Due to the rapid expansion of CAV vehicle technology use, the coexistence of HuD with AuD on shared roadways have been studied extensively over the last few years. Liu et al. [24] proposed comprehensive instruction for modeling mixed traffic on multilane freeway facilities. This study specifically looked into mobility improvements brought upon by the introduction of AuD, warranting further study on fundamental features of mixed traffic. The authors were influenced by the modeling structure proposed in this study but pivoted the study focus towards macroscopic correlations of flow-density. An analytical capacity model was proposed by Gjaisi et al. [25] for mixed traffic. This study examined the different mixed traffic scenarios (i.e., varying demand, market shares, platooning, and technology use) to determine optimal AuD vehicle lanes for maximizing mixed traffic throughput. Based on a similar goal, Chen et al. [26] developed a general formulation to estimate the capacity of mixed traffic based on vehicle spacing, platoon configurations, and AuD shares. Gong and Du [27] developed a

cooperative platoon control based on a model predictive control strategy for mixed traffic that focused on reducing oscillation propagation and stabilizing traffic flow. A simulation-based traffic state estimation study was executed by Fountoulakis et al. [28] that demonstrated satisfactory estimation results for varying traffic state and penetration rates. Talebpour and Mahmassani [29] developed a simulation framework to analyze overall stability and throughput at different mixed traffic conditions. Additionally, the coexistence of HuD and AuD were found to be effective in preventing shockwave formation and propagation. Deng [30] proposed a simulation framework of mixed traffic incorporating human driving behavior from VISSIM and Adaptive Cruise Control and Cooperative Adaptive Cruise Control models from Van Arem et al. [31]. Ye and Yamamoto [32] proposed a modeling strategy to study the impact of dedicated AuD lanes on traffic flow throughput.

What is evident from the literature review is that a need exists to connect microscopic models with macroscopic models for both traditional and mixed traffic scenarios. While microscopic models could be accurate, to some extent, in estimating an individual vehicle's movement, the fit of these models to macroscopic scale requires significant extrapolation. Furthermore, although mixed traffic dynamics modeling has initiated considerable research efforts recently, major theoretical aspects that understand the true potential of CAV technology are yet to be explored. Critical reservation of mixed traffic-related studies would be a complete dependence on car-following models of hypothetical single-lane roadways. Hence, developing a traffic flow model that can incorporate the implications of complete motion dynamics of traffic movements will be the initial focus of this study and a significant effort to address the aforementioned shortcomings. At the same time, this study will present realistic, multilane, complex motion dynamics of both vehicle types and explore the resulting implications on the flow-density diagram, an important step in the study. Altogether, this study will attempt to specify the limitations of partial motion dynamics on a macroscopic scale and provide a reasonable approach to overcome those limitations.

3. Microscopic Modeling Framework of Mixed Multilane Traffic

To meet the developed objectives, we performed numerical simulations of 22 vehicles in a hypothetical homogenous two-lane roadway segment in MATLAB. At the beginning of the simulation, the number of vehicles varied between 8–12 vehicles in each lane. Significantly for our study, the simulated environment developed complete motion dynamics that included car-following, lane-changing, and gap-acceptance rules for individual vehicles corresponding to the vehicle type. All vehicles in the simulation revised their acceleration, lane-changing, and gap-acceptance decisions at each time-step with response to the surrounding vehicles' relative positions and velocities. Each simulation time-step duration was taken as 0.1 second (sec) of real-world time, and the simulation length was 9001 time-steps (0 to 9000) totaling 15 minutes of duration. First, two control-vehicles, one in each of the two lanes, followed a predefined acceleration profile. At the beginning of the simulation (0 time-step), all vehicles were placed on the roads by uniformly spacing them according to a simulated flow rate (from 1000 vehicles per hour to 2600 vehicles per hour) at 90 kilometers per hour (kph). The acceleration profiles of each lead vehicle were formed to generate bottlenecks for the following vehicles in each lane. At the 3001 time-step, the lead vehicles of each lane decelerated at the rate of -2 meter/sec^2 (m/s^2) to drop the speed of vehicles from 90 kph to 30 kph. This speed drop created an intentional bottleneck on the roadway segment where the following vehicles in each lane were unable to pass the lead vehicles. This provided an important opportunity to explore congested traffic states. Then, at the 4917 time-step, both lead vehicles accelerated at the rate of 2 m/s^2 to regain the speed from 30 kph to 90 kph.

3.1. Car-following Principles. Car-following, being the predominant maneuver during driving, has a greater influence on traffic states. In the proposed modeling framework, the car-following principles of vehicles primarily relied on paired vehicle types (e.g., HuD, AuD) of a subject vehicle and corresponding lead vehicle in the same lane of that subject vehicle. The HuD subject vehicles maintained the car-following IDM [2] irrespective of the lead vehicles type (i.e., HuD or AuD) for car-following maneuvers. The AuD vehicles adhered to car-following rules (i.e., Adaptive Cruise Control (ACC) and Cooperative Adaptive Cruise Control (CACC)) in response to the lead vehicle's type. If the lead vehicle was a HuD vehicle, then the AuD vehicles would follow ACC with relatively higher safety headway. Otherwise, the HuD vehicle would choose CACC and try to form a CACC platoon of AuD vehicles with the lead vehicle. The ideal ACC/CACC car-following model and parameter values were adopted from the work of Hu et al. [33]; an AuD vehicle would prefer to form CACC platoon with other AuD vehicles in the traffic stream. Platoon formation depended on the platoon configuration (i.e., intraplatoon headway, interplatoon headway, and maximum platoon length) (detailed descriptions of different platoon configurations and principles are available in the work of Seraj et al. [34]). Influenced by the findings from Seraj et al. [34], the present study employed a fixed platoon configuration (i.e., intraplatoon headway = 0.50 sec, interplatoon headway = 2.0 sec, and max. platoon length = 5 vehicles) to attain optimal mobility and safety benefits in mixed traffic environments.

In addition to usual car-following models, our modeling framework adopted a few subjective car-following models acquired from the IDM and ACC. The purpose of introducing these additional car-following models was to ensure a smooth adjustment to accommodate other two maneuvers (i.e., lane-changing and gap-acceptance) of vehicle motion dynamics. The preceding car-following (PCF) model was triggered for a subject vehicle prior to lane-changing when the vehicle was to change lanes but could not execute the maneuver due to lack of an adequate gap in the target lane. By contrast, the succeeding car-following (SCF) model was

activated to facilitate a subject vehicle's transition from the PCF principle right after the lane-changing maneuver. The accommodative car-following (ACF) model was used to enable a subject vehicle to increase spacing with its lead vehicle and accept a lane-changing vehicle from the nearby lane. The maximum duration a vehicle could remain in PCF, SCF, or ACF was chosen to be 5 sec (50 time-steps). Each vehicle had an acceleration equation specific to its' car-following state for each time-step. Relevant formulae to simulate vehicle movements are provided in Figure 1(a).

3.2. Lane-Changing Principles. The complex elements of motion dynamics (i.e., lane-changing and gap-acceptance) for vehicles had restricted application on the developed simulation structure. For HuD vehicles, only discretionary lane-changing that was motivated to gain free-flow speed was considered for modeling in this simulation. If a HuD vehicle were to drive below free-flow speed for 5 consecutive seconds, the vehicle driver would indicate the intention to change lane and start checking for an acceptable safety gap in the target lane. As for AuD vehicles, lane-changing intentions were only triggered by the possibility to form a CACC platoon with the lead vehicle in the target lane. However, an AuD vehicle would not intend to change lanes if it were already a part of the platoon. Both lane-changing and gap-acceptance rules developed for simulation were influenced by strategies proposed by Liu et al. [35] for mixed traffic movements. While the intentions for lane changes were conveyed as soon as the requirements were fulfilled, execution of lane-changing operations only occurred once the available gap in the target lane was governed by the gap-acceptance principles for respective vehicle types. In mixed traffic scenarios, vehicles were assigned with a Platoon Position ID (P^2ID) that indicated whether the vehicle was a part of CACC platoon, as well as identifying their physical position in that platoon. The P^2ID for all HuD vehicles was assigned as zero (0). AuD vehicles' P^2ID derived from the lead vehicle's type and P^2ID. For instance, if the lead vehicle in the same lane was a HuD vehicle, then the AuD vehicle's P^2ID would be one "1," and it would follow ACC car-following rules. However, if the lead vehicle was an AuD vehicle, then the subject AuD vehicle would form a CACC platoon with the lead vehicle, and a P^2ID would be assigned to the subject AuD vehicle according to the CACC platoon configuration (i.e., maximum platoon length). In another scenario, if the lead vehicle in the lane of an AuD vehicle were a HuD vehicle and the lead vehicle in the target lane was an AuD vehicle, the subject vehicle would attempt lane-changing from the current lane to the target lane, and the following vehicle in the target lane would try to safely receive the subject vehicle.

Since the motivation for discretionary lane-changing is not as strong as mandatory lane-changing, a conservative approach was taken to estimate required clearance for the maneuver by discounting extreme braking scenarios. A gap-searching subject vehicle would execute a lane-changing maneuver by implementing the following acceleration equation based on the vehicle type and start SCF from the next time-step.

$$a_{LC}(t) = \begin{cases} a_{\max}\left[1 - \left(\dfrac{v(t-1)}{v_f}\right)^4 - \left(\dfrac{s_0 + \max\left[0,\ v(t-1) \times T' + \left((v(t-1) \times \Delta v(t-1))/2\sqrt{a_{\max} b}\right)\right]}{s(t-1)}\right)^2\right], & \text{(for HuD)}, \\ k_1\left[\Delta p(t-1) - v(t-1) \times T' - s_0\right] + k_2 \Delta v(t-1), & \text{(for AuD)}, \end{cases} \tag{1}$$

and within 5-seconds of a lane-changing operation, the subject vehicle would reclaim its actual safety headway (T) and transfer to the car-following state according to the vehicle type and lead vehicle type. Meanwhile, the following vehicle would start adjusting the spacing with a new lead vehicle right after the lane-changing by the subject vehicle. A complete motion dynamic modeling scheme for both HuD and AuD vehicles are presented in Figures 1(b) and 1(c).

3.3. Gap-Acceptance Principles. The gap-acceptance of discretionary lane-changing for both vehicle types was based on the minimum accepted gap by the driver if the driver chose to merge into an available gap in the target lane. This gap must meet the following conditions to be considered a possibility for lane-changing by the subject vehicle:

$$\begin{aligned} G_{s,\min} &\geq 2g_0 + L, \\ G_{l,\min}, G_{f,\min} &\geq g_0. \end{aligned} \tag{2}$$

Here, $(G_{s,\min})$ = minimum total clearance in the target lane, $(G_{l,\min})$ = minimum lead clearance, and $(G_{f,\min})$ = minimum following clearance. Upon satisfying the minimum boundary conditions, the total available clearance in the target lane, between the lead and following vehicles, would be compared with the acceptable gap of the subject vehicle for the corresponding time-step. If the subject vehicle had a total gap in the target lane smaller than an acceptable lane-changing gap, the subject vehicle would move to PCF (provided that the vehicle was not in PCF for last 5-second time-step). The subject vehicle would stay on PCF for the maximum 5-second time-step and actively examine the available gap in the target lane to execute a lane-changing

- Intelligent driver model (IDM)

$$a(t) = a_{\max}\left[1 - \left(\frac{v(t-1)}{v_f}\right)^4 - \left(\frac{s_0 + \max\left[0, v(t-1)\times T + \frac{v(t-1)\times \Delta v(t-1)}{2\sqrt{a_{max} b}}\right]}{s(t-1)}\right)^2\right]$$

$a(t)$ = acceleration at time step t
$a_{\max}$ = maximum acceleration, 2.5 m/s^2
$v(t-1)$ = speed at time step $(t-1)$
v_f = free flow speed
s_0 = minimum spacing (7.5 m) = $g_0 + L$
g_0 = jam clearance, 2 m
L = average vehicle length, 5.5 m
$\Delta v(t-1)$ = speed difference with lead vehicle at $(t-1)$
b = desirable deceleration, 2.5 m/s^2
$s(t-1)$ = clearance with lead vehicle at $(t-1)$
T = safety head way, for a HuD vehicle T is fixed throughout the simulation period and varied randomly from 2 to 3 sec.

- Adaptive cruise control (ACC)
  $a(t) = k_1[\Delta p(t-1) - v(t-1)\times T - s_0] + k\Delta v(t-1)$
  k_1, k_2 = control constants for relative distance and relative velocity respectively ($k_1 = 0.3$, $k_2 = 0.5$)
  T = safety headway = 1.5 sec for vehicles at ACC
- Cooperative adaptive cruise control (CACC)
  $a(t)$ = same as ACC with T (safety headway) according to Intra/Inter platoon headway

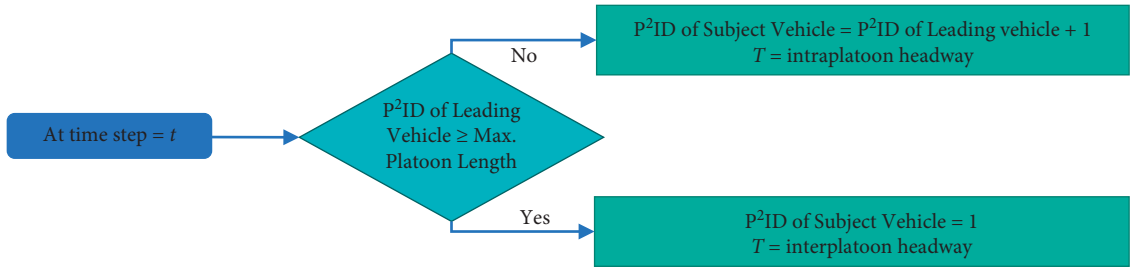

- Preceding car-following (PCF)
  - ✓ For HuD
    $a(t)$ = same as IDM
  - ✓ For AuD
    $a(t)$ = same as ACC

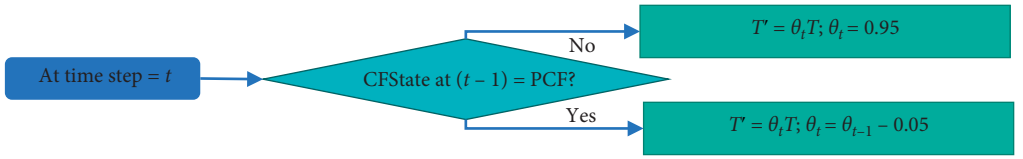

- Succeeding car-following (SCF)
  - ✓ For HuD
    $a(t)$ = same as IDM
  - ✓ For AuD
    $a(t)$ = same as ACC

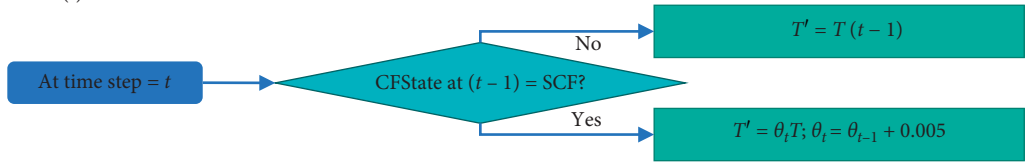

- Accommodating car-following (SCF)
  - ✓ For HuD
    $a(t)$ = same as IDM
  - ✓ For AuD
    $a(t)$ = same as ACC

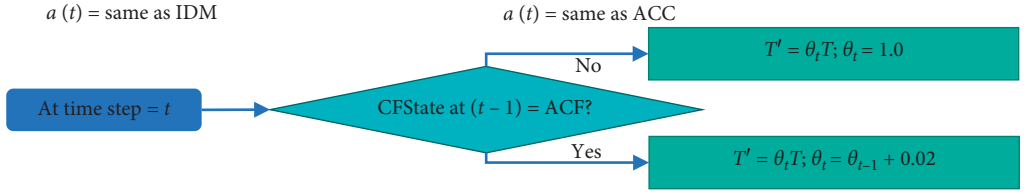

- Lane-changing (LC)
  - ✓ For HuD
    $a(t)$ = same as IDM
  - ✓ For AuD
    $a(t)$ = same as ACC

(a)

Figure 1: Continued.

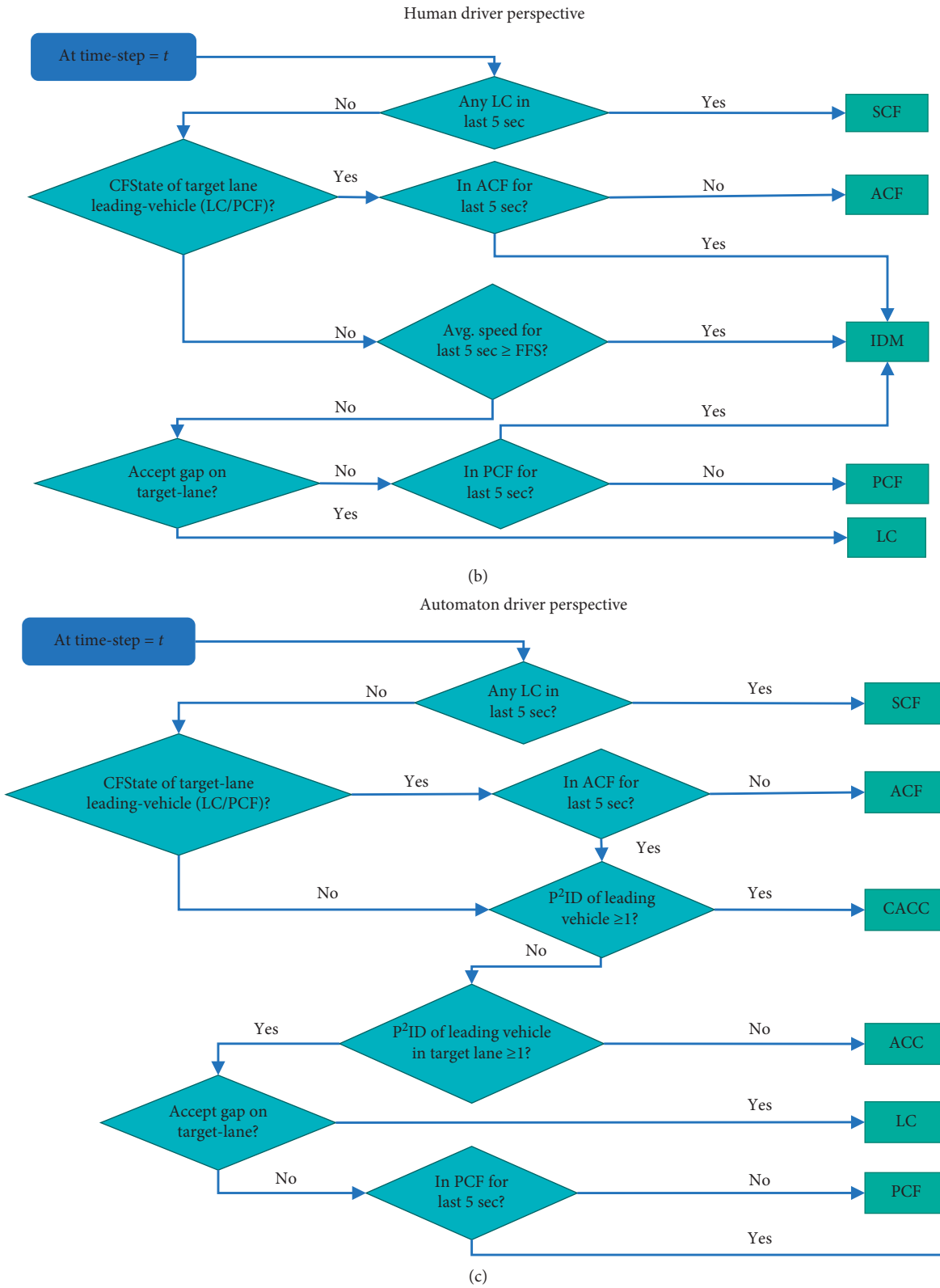

Figure 1: (a) Implemented formulae for the modeling framework, (b) principles for a human driver, and (c) principles for an automaton driver to model multilane traffic movements.

operation. If the vehicle could not find an acceptable gap within this 5-second time-step in PCF, it would move back to the primary car-following mode (i.e., IDM, ACC). The subject vehicle would, then, seek the following conditions to identify an acceptable gap ($G_{s,\text{acc}}$) for lane-changing at any time-step:

$$\begin{aligned} G_{s,\text{acc}}(t') &= \max\left\{G_{s,\min}, G_{s,\text{req}}(t')\right\}, \\ G_{s,\text{req}}(t') &= \left[v_s(t') + \Delta v_f(t')\right]T_s' + \left[v_s(t') + \Delta v_l(t')\right]T_s' + L, \\ \Delta v_l &= \left[v_s(t') - v_l(t')\right], \\ \Delta v_f &= \left[v_s(t') - v_f(t')\right], \end{aligned} \tag{3}$$

where $G_{s,\text{acc}}$ = acceptable clearance, t' = time-step in PCF, s = subject vehicle, l = lead vehicle in the target lane, f = following vehicle in the target lane, $G_{s,\text{req}}$ = required clearance, Δv = speed difference, and T_s' = modified safety headway of the subject vehicle.

Similarly, if a subject vehicle observed that a lead vehicle in a neighbour lane had activated PCF (assumed to be conveyed by indicator light), the subject vehicle would move to the ACF mode for a maximum 5-second time-step to receive that vehicle as a new lead vehicle. Upon successful lane-changing by the lead vehicle in the target lane within the 5-second time-step, the subject vehicle would shift to the PCF mode specific to the vehicle type. Otherwise, the subject vehicle would automatically move back to the primary car-following mode (i.e., IDM, ACC) after the 5-second time-step in ACF. Within this 5-second window, the safety headway (T') for the subject vehicle would change gradually to allow for a smaller acceptable gap for lane-changing (in PCF) to broaden the gap between the lead vehicle and itself in the same lane to accommodate the lane-changing of the lead vehicle from a neighbor lane (in ACF) and to increase the gap between a new lead vehicle (in SCF) and itself. The safety headway would meet the conditions mentioned in Figure 1(a), specific to subjective car-following modes. If a vehicle can successfully execute a lane-changing maneuver, the vehicle would shift to SCF in the following time-step and stay on that mode until it reclaimed its initial safety headway (T).

4. Flow-Density Relationships for a Human-Driven Vehicle

4.1. Limitations of the Macroscopic Adaptation of the Car-following Model. In a real-world scenario, car-following action is the most frequent task performed by drivers in vehicle motion. Therefore, the amplification of a microscopic car-following model for homogenous traffic in a state of steady equilibrium should provide an ideal representation of the fundamental diagram. In this regard, the IDM was expanded to obtain traffic flow models between speed and density. The following forms of equation were obtained [18]:

$$\begin{aligned} k &= \frac{1}{(s_0 + vT)\left[1 - \left(v/v_f\right)^{\delta}\right]^{-(1/2)}}, \\ v &= v_f\left[1 - \left(\frac{k}{k^*}\right)^2\right], \\ q &= \frac{v}{(s_0 + vT)\left[1 - \left(v/v_f\right)^{\delta}\right]^{-(1/2)}}, \end{aligned} \tag{4}$$

where k = mean density, s_0 = minimum spacing, v_f = free-flow speed, k^* = desired mean density, and q = mean traffic flow. The macroscopic form of the IDM involved four parameters (i.e., v_f, s_0, T, δ) that determine the shapes and features of fundamental relations (i.e., flow, speed, and density). To check the capability of the derived macroscopic model to explain these relations, a wide range of traffic flow scenarios (i.e., flow rates = 1000 vph–2600 vph) was simulated under the proposed modeling framework containing only HuD vehicles in the traffic stream. Measured outputs from the simulations were computed and calibrated to obtain flow-density values and model parameters, respectively. Macroscopic parameter values were measured according to the techniques proposed in the Highway Capacity Manual [36]. Flow and respective density values for different simulated traffic flow scenarios are plotted in Figure 2. The macroscopic form of the IDM is also plotted in the same figure with the premeditated parameter values (i.e., $(s_0 = 7.5\,\text{m},\ v_f = 90\,\text{kph},\ T = 1.98\,\text{sec},\ \delta = 4)$ used for the simulation.

Since the parameters required to generate the Fundamental Diagram (FD), derived from the IDM, were obtained from the parameters provided as inputs of the car-following IDM in the simulation, calibration of the parameters was exempt. Therefore, the FD obtained from the given parameter set should represent the real-world implications of an expanded IDM on the flow-density relation. However, as observed in Figure 2(a), the plotted FD, derived from IDM, did not capture the extremity and variations observed from the simulated flow-density results. Analysis of the simulated traffic's microscopic features revealed that, for 90.73% of the total duration, the vehicles maintained the car-following state (i.e., IDM). The remaining share of vehicle movements was spent on lane-changing-related motion dynamics (i.e., LC, PCF, SCF, and ACF). The comparison between the flow-density points from the simulation with the generated FD revealed that the lane-changing gap-acceptance control decisions had an influential impact from a macroscopic perspective. While car-following was a predominant maneuver on the microscopic scale, the impact of lane-changing gap-acceptance was far more significant from a macroscopic viewpoint.

To further investigate the capability of the FD derived from the IDM, we explored empirical data obtained from a recurrent bottleneck segment of an urban freeway corridor: Whitemud Drive, Edmonton, Canada. Whitemud Drive is a multilane freeway with a posted speed limit of 80 kph and

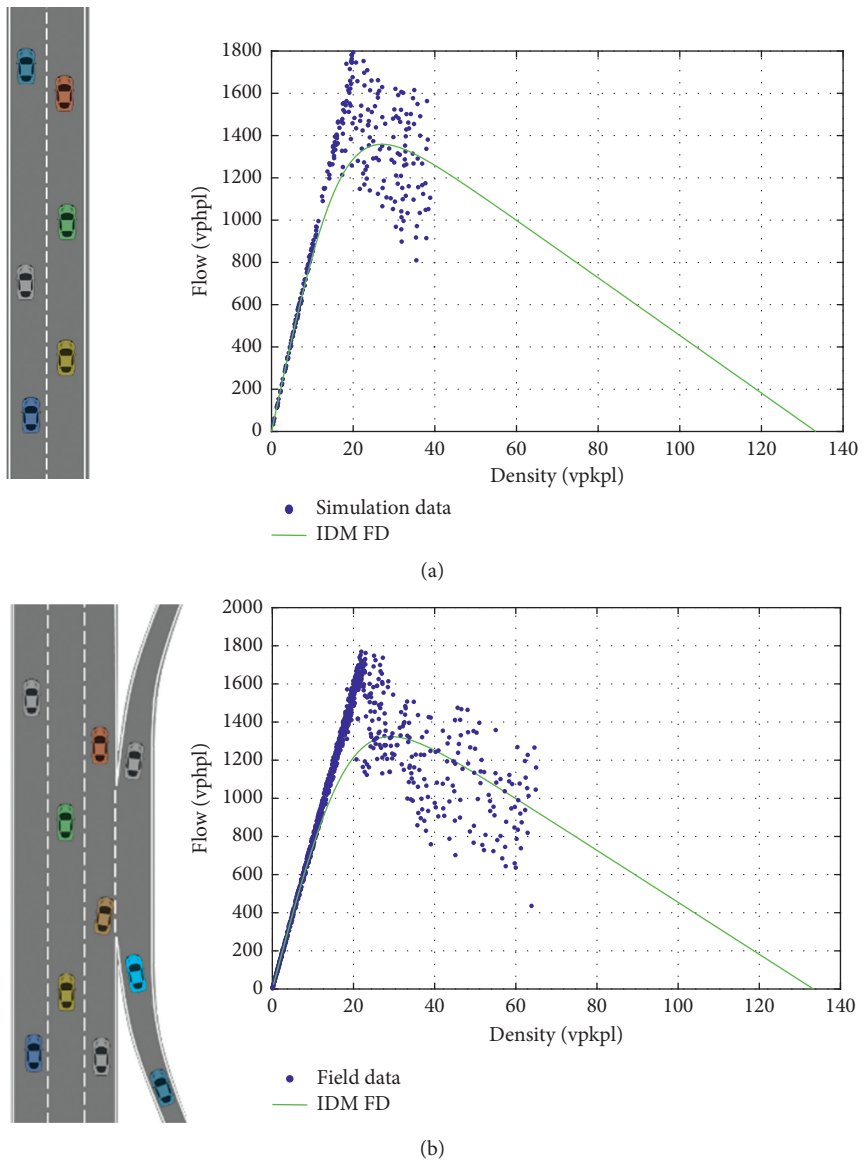

Figure 2: Resulting fundamental diagrams by the macroscopic IDM from (a) simulation data and (b) empirical data.

serves as a part of Edmonton's inner ring road. The annual, average daily traffic (AADT) of its westbound section was greater than 100,000 vehicles in 2017 [37]. For the study purpose, we have used 24 hr data from 30 workdays (from August 7, 2017, to September 18, 2017). Based on field observations and bottleneck information, the weaving segment after the 122 Street on-ramp and the segment around Fox Drive were selected as critical segments for this study. The selected segments were, then, equipped with loop detectors on each lane to collect traffic flow data (i.e., speed, flow, and occupancy) at 20-second intervals. The studied roadway segment had four (4) lanes with a one-lane on-ramp at the beginning and a one-lane off-ramp at the end of the segment. The free-flow speed for the FD was taken to be 80 kph since this was the maximum speed limit of the freeway. The minimum spacing was taken as 7.5 m (5.5 m (average vehicle length) + 2 m (safety clearance)), and $\delta = 4$ was considered. The safety headway ($T = 1.98$ sec) for traffic was calibrated for the FD using empirical data points. Analogous to earlier observations, the FD failed to capture the entirety of the fundamental relation between flow and density. The FD provided a lower capacity value and failed to explain the capacity drop phenomenon. Therefore, traffic flow models, by expanding the car-following dynamic, do not adequately explain most of the traffic flow states and events. While the microscopic car-following model considered vehicle-to-vehicle interactions in the same lane, this model failed to apprehend interactions of vehicles in multiple lanes. As such, FDs derived from car-following models cannot be expected to comprehensively interpret traffic flow characteristics. In that context, a macroscopic model can only consider safety spacing during car-following and accommodate speed, as well as space sensitivity, from drivers relevant to lane-changing and gap-acceptance.

4.2. Proposed Traffic Flow Model. Premised on these findings, a new, flexible, and integrated traffic flow model can now be formulated. In general, the proposed model must consist of a safety spacing principle, predominant in car-following dynamics, while integrating broad-scale speed and space sensitivity, which are prevailing aspects on lane-changing and gap-acceptance. These considerations are incorporated when reviewing numerous forms of traffic flow and result in the following formulation:

$$k = \frac{1}{\left(\left(s_0 + vT + \lambda v^2\right)\left[1 - \ln\left(1 - \left(v/v_f\right)\right)\right]^{(1/\eta)}\right)},$$

$$v = v_f\left[1 - e^{\{1-(k^*/k)\}^{\eta}}\right], \tag{5}$$

$$q = \frac{v}{\left(\left(s_0 + vT + \lambda v^2\right)\left[1 - \ln\left(1 - \left(v/v_f\right)\right)\right]^{(1/\eta)}\right)},$$

where v = mean speed of traffic, v_f = free-flow speed, k = mean density, and k^* = the desired mean density. The latter, considering traffic safety rules, then takes the following form:

$$k^* = \frac{1}{s_0 + vT + \lambda v^2}. \tag{6}$$

Here, λ = represents the awareness of the mean speed of traffic; T = the mean safety headway of the driving population; s_0 = minimum spacing; and η = represents sensitivity to the average spacing of traffic.

Since simulated, discretionary lane-changing was assumed to be motivated by speed gain and successful lane-changing maneuvers depend on the available spacing between vehicles, and the new parameters (i.e., λ and η) should account for and relate to the lane-changing of vehicles in traffic.

4.3. Differentiability of the Proposed Traffic Flow Model. The ability of the proposed model to explain the flow-density relationship can be further analyzed to generate sensible information. For instance, one can take the first derivatives of flow (q) with respect to velocity (v) to find the capacity and set the result to zero.

$$\frac{dq}{dv} = k + v\frac{dk}{dv} = v\left[-\frac{(T + 2\lambda v)\left[1 - \ln\left(1 - \left(v/v_f\right)\right)\right]^{-(1/\eta)}}{\left(s_0 + vT + \lambda v^2\right)^2} - \frac{\left[1 - \ln\left(1 - \left(v/v_f\right)\right)\right]^{-1-(1/\eta)}}{\eta v_f\left(1 - \left(v/v_f\right)\right)\left(s_0 + vT + \lambda v^2\right)}\right] + \frac{\left[1 - \ln\left(1 - \left(v/v_f\right)\right)\right]^{-(1/\eta)}}{\left(s_0 + vT + \lambda v^2\right)}. \tag{7}$$

Additionally, the traffic flow (q) can be differentiated with respect to density (dq/dk) to obtain the slope of a tangent at any point on a flow-density curve. Hence,

$$\frac{dq}{dk} = v + k\frac{dv}{dk} = v + \frac{k}{(dk/dv)}$$

$$= \frac{\left[1 - \ln\left(1 - \left(v/v_f\right)\right)\right]^{-(1/\eta)}}{\left(s_0 + vT + \lambda v^2\right)\left[-\left(\left((T + 2\lambda v)\left[1 - \ln\left(1 - \left(v/v_f\right)\right)\right]^{-(1/\eta)}\right)/\left(s_0 + vT + \lambda v^2\right)^2 - \left(\left[1 - \ln\left(1 - \left(v/v_f\right)\right)\right]^{-1-(1/\eta)}/\eta v_f\left(1 - \left(v/v_f\right)\right)\left(s_0 + vT + \lambda v^2\right)\right)\right]} + v. \tag{8}$$

Moreover, as a boundary condition of the flow-density relationship, shockwave speed (w_j) at density can be determined from the abovementioned equation:

$$w_j = \frac{dq}{dk}\Big|k = k_j, v = 0 = -\frac{s_0}{T + \left(s_0/\eta v_f\right)}. \tag{9}$$

4.4. Sensitivity of the Proposed Traffic Flow Model Parameters. An expected feature of the traffic flow model is the flexibility to explain different shapes of fundamental diagrams from a single model. Two additional parameters introduced in the proposed model (i.e., λ and η) provide greater flexibility and precision in replicating wide variations of flow-density relationships. Figure 3 illustrates a group of fundamental diagrams generated from the proposed model with varying speed and spacing sensitivity parameters. Figure 3 establishes that both speed and spacing sensitivity can effectively influence the shape of the flow-density relationship and produce diverse shapes based on empirical data. However, the interaction of speed and spacing sensitivity with other parameters in the model requires further analysis.

4.5. Applicability on Simulated and Empirical Observations. With the potential of the proposed model now established, its proficiency in portraying fundamental features of traffic,

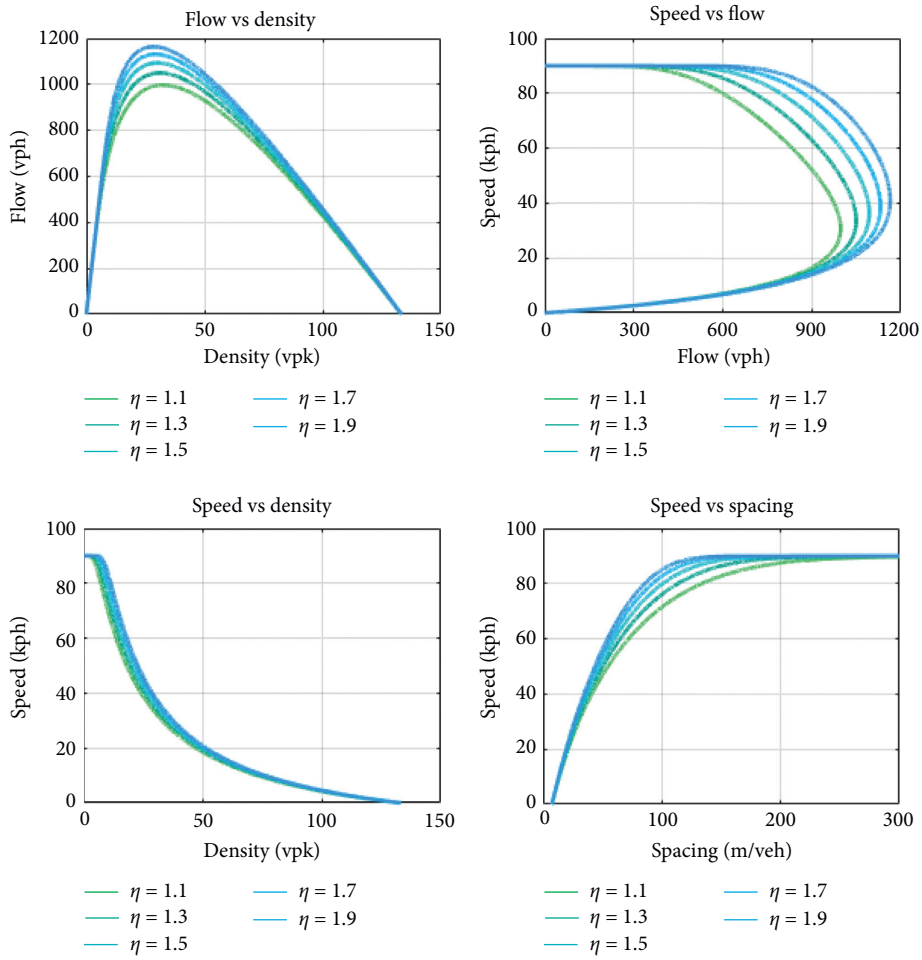

(a)

Figure 3: Continued.

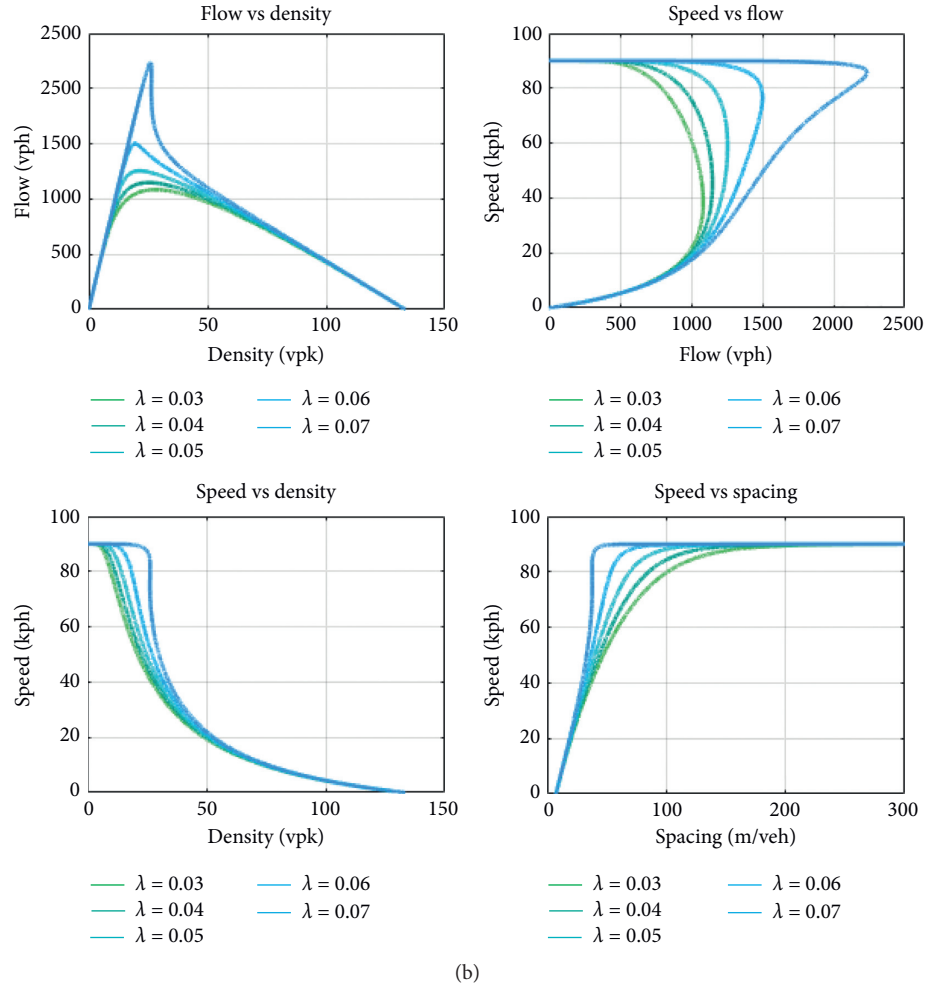

(b)

Figure 3: Variability of the fundamental diagram resulting from changes in the (a) spacing sensitivity parameter and (b) speed sensitivity parameter.

for both simulated and empirical data, was tested and compared with the macroscopic IDM. Common parameters for both models (i.e., $s_0 = 7.5$ m, $v_f = 90$ kph, and $T = 1.98$ sec) were maintained for fundamental diagram calibration. As shown in Figure 4, the fundamental diagrams generated through the proposed model were a better fit than the macroscopic extrapolation of the IDM. The Root Mean Square Error (RMSE) was reduced by 42.67% for the simulation data and by 37.41% for the field data in comparison to the IDM. Additionally, the congestion element to the fundamental diagram of the proposed model had curvilinear shapes that were instrumental in explaining the capacity drop phenomenon. A similar output was experienced for empirical observations, which established the absolute superiority of the proposed model over macroscopic adaptation of the IDM with respect to the competence of explaining traffic flow features.

4.6. Flow-Density Relationship for Mixed Traffic. The capability of the proposed model to apprehend the macroscopic implications of complete motion dynamics has been established in the previous section of this paper. We will now explore the model's adeptness to explain flow-density relationships for different mixed traffic scenarios and correlations of model parameters with AuD vehicle shares and lane-changing rates in this section. Our mixed traffic scenarios, for this study, were developed considering different AuD vehicle shares in simulated traffic while adhering to the aforementioned traffic dynamic principles (i.e., car-following, lane-changing, and gap-acceptance) according to vehicle types (i.e., AuD and HuD vehicle). The obtained results from the simulation were utilized to calibrate the model parameters and plot the flow-density diagrams for different mixed traffic conditions; Table 1 and Figure 5. The flexibility of the proposed model allowed for more precise replication of a wide variety of fundamental relations. Additionally, both parameters introduced in the proposed model demonstrated their sensitivity to different traffic conditions.

As described in the section on the microscopic modeling framework of mixed multilane traffic, two types of vehicle were simulated by following the developed car-following, lane-changing, and gap-acceptance principles for varying flow rates (i.e., 1000–2600 vphpl) and specific AuD vehicle shares. Microscopic parameters of individual vehicles were

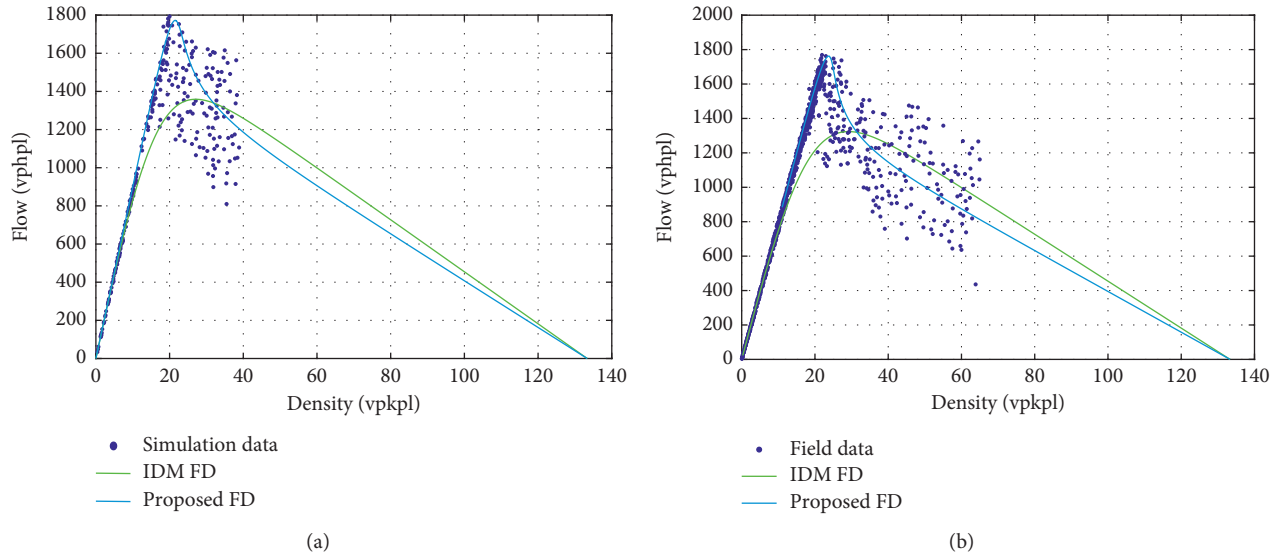

Figure 4: Comparison of the calibrated fundamental diagrams resulting from the macroscopic IDM and proposed traffic flow model on (a) simulation data and (b) empirical data.

Table 1: Model parameters of the proposed model for distinct mixed traffic scenarios.

AuD share (%)	s_0 (m)	v_f (kph)	T (sec)	λ (s^2/m)	η
0	7.5	89.86	1.98	−0.0668	1.349
25	7.5	87.89	1.76	−0.0617	1.401
50	7.5	88.16	1.46	−0.0523	1.470
75	7.5	88.50	1.31	−0.0447	1.690
100	7.5	90.00	1.18	−0.0394	1.849

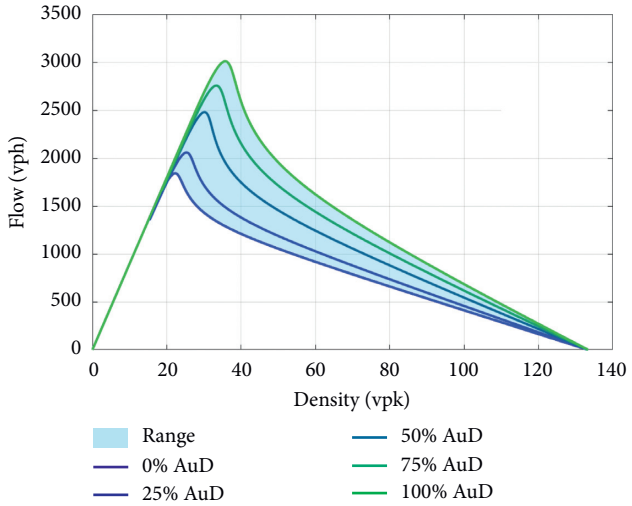

Figure 5: Resulting fundamental diagrams for distinct mixed traffic conditions generated from numerical simulations.

recorded throughout the simulation period for specific simulation scenarios (i.e., flow rate and AuD share). These parameters included position, velocity, acceleration, and current lane. The average number of lane changes by the vehicles in traffic was measured from assessing these features. This average was presumed to have a notable influence on traffic flow and was, therefore, measured for each simulation scenario. The recorded microscopic features were, then, translated into macroscopic traffic flow parameters for the simulated roadway segment. The flow, density, and average speed of traffic were calculated from microscopic data for specific AuD market shares and plotted to develop a traffic condition-specific flow-density diagram Figure 5. The calibrated flow-density curves demonstrated the combinatorial impact of introduced parameters (i.e., λ and η) in effectively portraying the correlation between traffic flow parameters.

To demonstrate the implications of lane-changing on mixed traffic scenarios, the interactions of the lane-changing rate with increasing traffic flow rates were assessed. The lane-changing rate (number of lane changes/minute) of traffic was measured by counting the total number lane changes by simulated traffic (22 vehicles) over the simulation period in minutes (15 minutes). The simulated environment provided the opportunity to precisely measure every instance of lane-changing by the vehicles and otherwise a difficult task when working with real-world traffic. Results showed a strong linear correlation of the lane-changing rate with increasing flow rates Figure 6. The observations outlined in Figure 6 show the regression line for 0% displaying an upward trend with increasing flow rates. However, the higher residuals indicated an unstable correlation between the variables at 0% AuD traffic. Further analysis demonstrated a reduction in residual values with an increased number of AuD vehicles in traffic. Moreover, a gradual decrease in the lane-changing rate with increased AuD vehicle shares was observed. Although the extent of reduction in lane-changing rates varied for different flow rates, the trend of diminishing lane-changing was notable. The result of this particular analysis warrants future examination of lane-changing demand and supply equilibrium in different mixed traffic scenarios.

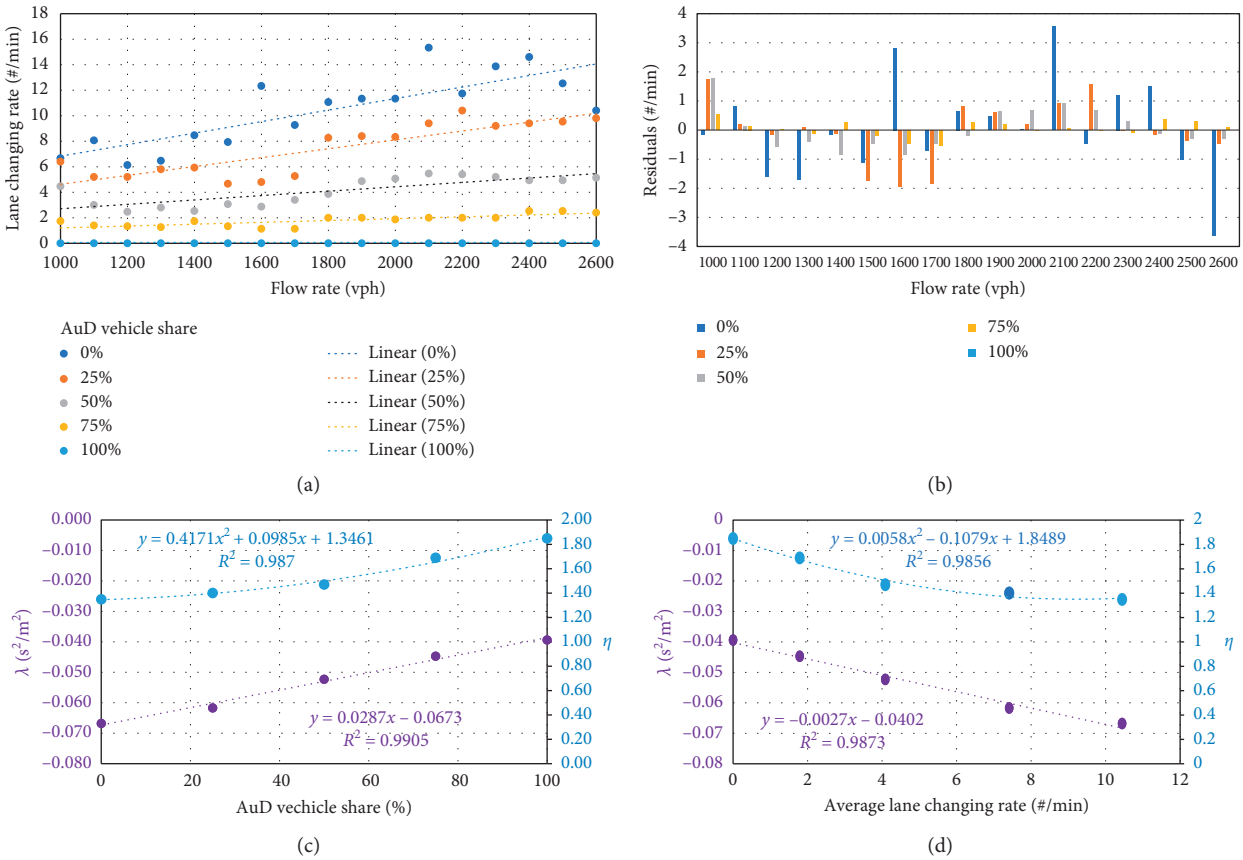

FIGURE 6: (a) Patterns of lane-changing rates, (b) regression residuals with increasing traffic flow rates at increasing flow rates for different mixed traffic conditions, (c) interactions of the introduced model parameters with AuD vehicle shares in traffic, and (d) average lane-changing rates.

To justify the inclusion of speed and space sensitivity in the traffic flow model, the correlation of both parameters with changing traffic conditions was analyzed. Analysis of the flow-density relationship in mixed traffic scenarios demonstrated the evolution of the fundamental diagram, plotted by the proposed macroscopic model, with an increasing share of AuD vehicles. While minimum spacing (s_0) was predefined for the simulation, free-flow speed (v_f) and safety headway of traffic (T) were computed from the simulation outcomes. Afterwards, the speed and spacing sensitivity parameter (λ and η) were calibrated to best fit the obtained flow-density points of different mixed traffic scenarios. This study used neutral regression by normalizing the RSME of two fundamental parameters (flow and density) to minimize overall errors. Analysis of the best fit of λ and η values uncovered their correlation with AuD vehicle shares; Figure 6(c). While λ was linearly correlated with the simulated mixed traffic scenarios (i.e., 0%, 25%, 50%, 75%, and 100% AuD vehicle shares), η showed a quadratic correlation with AuD vehicle shares. High R^2 values for both cases established a strong correlation between λ and η with AuD vehicles' presence in traffic. Further analysis of λ and η values at different AuD vehicle shares proved their association with lane-changing maneuvers; Figure 6(d).

5. Concluding Remarks

This paper has considered the fundamental drawbacks to the conversion of a microscopic model into a macroscopic model. In place of this, we have proposed an efficient, flexible traffic flow model that is capable of capturing limits and variations of fundamental diagrams. The proposed model is formulated by taking the impact of vehicles' complete motion dynamics into account. While the proposed model was portrayed in the macroscopic scale, it also balanced the microscopic vehicle dynamics through speed and spacing sensitivity parameters that gave the model better adaptability to recognize the fundamental features with greater precision. Proficiency of the proposed model was compared with the macroscopic car-following model by fitting both simulation and empirical data. The flexibility of the proposed model was also evaluated by calibrating the model parameters to shape the fundamental diagrams for different mixed traffic conditions.

Considering the magnitude of research warranted by the identified issues from previous research, this study makes notable contributions to the transportation literature by (i) revealing the limitations of the macroscopic car-following model to explain the fundamental features of multilane traffic flow, (ii) establishing the prominence and capability of

a single-regime equilibrium traffic flow model to account for the complete motion dynamics of traffic, (iii) capturing the variations of the fundamental diagram with different mixed traffic scenarios through single traffic flow models, and (iv) explaining the correlation of model parameters with vehicle motion dynamics and AuD shares on traffic. Given these key contributions, the most substantial theoretical significance of this study is in addressing the highly contested explanation of the macroscopic fundamental diagram by exploring the implications of the lane-changing maneuver. Although lane-changing has long been proposed as an elementary source of disturbance with broader consequences on traffic, surprisingly little empirical evidence that meets scientific standards was available to support this claim. Hence, this study carefully examined the macroscopic implications of complete motion dynamics to address the considerable gap in the existing body of knowledge. What we found was that incorporating the influences of bidirectional movements of traffic through speed and space sensitivity parameters would promote more accurate estimation of the fundamental diagram while providing adequate flexibility to adapt with varying mixed traffic scenarios.

The unique properties characterizing the proposed traffic flow model facilitate the replication of numerous traditional and mixed traffic scenarios. This substantially improved model can successfully explain the roadway capacity and capacity drop phenomenon, thus recognizing both opportunities and limitations of the roadway. Furthermore, leveraging the proposed model can facilitate more advanced and accurate highway performance functions to assist dynamic route choice on a traffic network. A future extension of this study will be to examine the applicability of the proposed model in signalized, arterial traffic and modifications required when considering the implications of a traffic signal on traffic flow. Besides, the lane-changing implications on traffic flow at varying mixed traffic scenarios will be further explored.

Data Availability

The simulated data used to support the findings of this study are available from the corresponding author upon request.

Conflicts of Interest

The authors declare that there are no conflicts of interest regarding the publication of this paper.

Acknowledgments

The authors want to acknowledge the support from the Natural Sciences and Engineering Research Council (NSERC) of Canada, City of Edmonton, and Transport Canada for funding this research. The contents of this paper reflect the views of the authors who are responsible for the facts and the accuracy of the data presented herein. The contents do not necessarily reflect the official views or policies of NSERC, City of Edmonton, and Transport Canada. The authors also acknowledge the contributions by Dr. Sharon Harper for her assistance in editing and proofreading the paper. This research work was jointly supported by the Natural Sciences and Engineering Research Council (NSERC) of Canada, City of Edmonton, and Transport Canada.

References

[1] SAE International, *AutoDrive Challenge*, SAE International, Warrendale, PA, USA, 2016, https://autodrivechallenge.com/.

[2] M. Treiber, A. Hennecke, and D. Helbing, "Congested traffic states in empirical observations and microscopic simulations," *Physical Review E*, vol. 62, no. 2, pp. 1805–1824, 2000.

[3] V. L. Knoop, *Introduction to Traffic Flow Theory: An Introduction with Exercises*, Delft University of Technology, Delft, Netherlands, 2017.

[4] B. D. Greenshields, J. R. Bibbins, W. S. Channing, and H. H. Miller, "A study of traffic capacity," *Highway Research Board Proceedings*, vol. 14, 1935.

[5] H. Greenberg, "An analysis of traffic flow," *Operational Research*, vol. 7, no. 1, pp. 79–85, 1959.

[6] G. F. Newell, "Nonlinear effects in the dynamics of car following," *Operational Research*, vol. 9, no. 2, pp. 209–229, 1961.

[7] L. C. Edie, "Car-following and steady-state theory for noncongested traffic," *Operational Research*, vol. 9, no. 1, pp. 66–76, 1961.

[8] B. S. Kerner and P. Konhäuser, "Structure and parameters of clusters in traffic flow," *Physical Review E*, vol. 50, no. 1, pp. 54–83, 1994.

[9] J. M. D. Castillo and F. G. Benítez, ""On the functional form of the speed-density relationship-I: general theory," *Transportation Research Part B: Methodological*, vol. 29, no. 5, pp. 373–389, 1995.

[10] N. Wu, "A new approach for modeling of fundamental diagrams," *Transportation Research Part A*, vol. 36, no. 10, pp. 867–884, 2002.

[11] Y. Ji, W. Daamen, S. Hoogendoorn, S. Hoogendoorn-Lanser, and X. Qian, "Investigating the shape of the macroscopic fundamental diagram using simulation data," *Transportation Research Record Journal of the Transportation Research Board*, vol. 2161, no. 1, pp. 40–48, 2010.

[12] H. Wang, J. Li, Q. Chen, and D. Ni, ""Logistic modeling of the equilibrium speed-density relationship," *Transportation Research Part A*, vol. 45, no. 6, pp. 554–566, 2011.

[13] J. Li and H. M. Zhang, "Fundamental diagram of traffic flow," *Transportation Research Record*, vol. 2260, no. 1, pp. 50–59, 2011.

[14] X. Wu, H. X. Liu, and N. Geroliminis, "An empirical analysis on the arterial fundamental diagram," *Transportation Research Part B*, vol. 45, no. 1, pp. 255–266, 2011.

[15] M. Keyvan-Ekbatani, A. Kouvelas, I. Papamichail, and M. Papageorgiou, "Exploiting the fundamental diagram of urban networks for feedback-based gating," *Transportation Research Part B: Methodological*, vol. 46, no. 10, pp. 1393–1403, 2012.

[16] M. Keyvan-Ekbatani, M. Papageorgiou, and I. Papamichail, "Urban congestion gating control based on reduced operational network fundamental diagrams," *Transportation Research Part C*, vol. 33, pp. 74–87, 2013.

[17] B. Coifman and S. Kim, "Extended bottlenecks, the fundamental relationship, and capacity drop on freeways," *Procedia Social and Behavioral Sciences*, vol. 17, pp. 44–57, 2011.

[18] D. Ni, *Traffic Flow Theory*, Elsevier, Amsterdam, Netherlands, 2016.

[19] A. Duret, C. Buisson, and N. Chiabaut, "Estimating individual speed-spacing relationship and assessing ability of newell's car-following model to reproduce trajectories," *Transportation Research Record: Journal of the Transportation Research Board*, vol. 2088, pp. 188–197, 2008.

[20] N. Chiabaut, L. Leclercq, and C. Buisson, "From heterogeneous drivers to macroscopic patterns in congestion," *Transportation Research Part B*, vol. 44, no. 2, pp. 299–308, 2010.

[21] D. Chen, S. Ahn, J. Laval, and Z. Zheng, "On the periodicity of traffic oscillations and capacity drop : the role of driver characteristics," *Transportation Research Part B*, vol. 59, pp. 117–136, 2014.

[22] M. Treiber and A. Kesting, "Microscopic calibration and validation of car-following models—a systematic approach," *Procedia Social and Behavioral Sciences*, vol. 80, pp. 922–939, 2014.

[23] J. Zheng, K. Suzuki, and M. Fujita, "Evaluation of car-following models using trajectory data from real traffic," *Procedia Social and Behavioral Sciences*, vol. 43, pp. 356–366, 2012.

[24] H. Liu, X. David Kan, S. E. Shladover, X. Y. Lu, and R. E. Ferlis, "Modeling impacts of cooperative adaptive cruise control on mixed traffic flow in multi-lane freeway facilities," *Transportation Research Part C*, vol. 95, pp. 261–279, 2018.

[25] A. Ghiasi, O. Hussain, Z. Sean Qian, and X. Li, "A mixed traffic capacity analysis and lane management model for connected automated vehicles: a markov chain method," *Transportation Research Part B*, vol. 106, pp. 266–292, 2017.

[26] D. Chen, S. Ahn, M. Chitturi, and D. A. Noyce, "Towards vehicle automation: roadway capacity formulation for traffic mixed with regular and automated vehicles," *Transportation Research Part B*, vol. 100, pp. 196–221, 2017.

[27] S. Gong and L. Du, "Cooperative platoon control for a mixed traffic flow including human drive vehicles and connected and autonomous vehicles," *Transportation Research Part B*, vol. 116, pp. 25–61, 2018.

[28] M. Fountoulakis, N. Bekiaris-Liberis, C. Roncoli, I. Papamichail, and M. Papageorgiou, "Highway traffic state estimation with mixed connected and conventional vehicles: microscopic simulation-based testing," *Transportation Research Part C: Emerging Technologies*, vol. 78, 2017.

[29] A. Talebpour and H. S. Mahmassani, "Influence of connected and autonomous vehicles on traffic flow stability and throughput," *Transportation Research Part C: Emerging Technologies*, vol. 71, pp. 143–163, 2016.

[30] Q. Deng, "A general simulation framework for modeling and analysis of heavy-duty vehicle platooning," *IEEE Transactions on Intelligent Transportation Systems*, vol. 17, no. 11, pp. 3252–3262, 2016.

[31] B. Van Arem, C. J. G. Van Driel, and R. Visser, "The impact of cooperative adaptive cruise control on traffic-flow characteristics," *IEEE Transactions on Intelligent Transportation Systems*, vol. 7, no. 4, pp. 429–436, 2006.

[32] L. Ye and T. Yamamoto, "Modeling connected and autonomous vehicles in heterogeneous traffic flow," *Physica A: Statistical Mechanics and its Applications*, vol. 490, pp. 269–277, 2018.

[33] S. G. Hu, H. Y. Wen, L. Xu, and H. Fu, "Stability of platoon of adaptive cruise control vehicles with time delay," *Transportation Letters*, vol. 7867, pp. 1–10, 2017.

[34] M. Seraj, J. Li, and T. Z. Qiu, "Modeling microscopic car-following strategy of mixed traffic to identify optimal platoon configurations for multiobjective decision-making," *Journal of Advanced Transportation*, vol. 201815 pages, Article ID 7835010, 2018.

[35] H. Liu, S. E. Shladover, X. Lu, and R. A. Ferlis, "Impact of cooperative adaptive cruise control (CACC) on multilane freeway merge capacity," in *Proceedings of the Transportation Research Board 97th Annual Meeting*, Washington, DC, USA, January 2018.

[36] Transportation Research Board, *HCM 2010 : Highway Capacity Manual*, Transportation Research Board, Washington, DC, USA, Fifth edition, 2010.

[37] E. O. F. Bear and H. Rd, *Alberta Highways 1 TO 986 Traffic Volume History 2006–2017*, Government of Alberta publications, Edmonton, Canada, 2018.